Cell

An EB1-Binding Motif Acts as a Microtubule Tip Localization Signal

Srinivas Honnappa,[1,6,7] Susana Montenegro Gouveia,[2,6] Anke Weisbrich,[1,6] Fred F. Damberger,[3,6] Neel S. Bhavesh,[3,8] Hatim Jawhari,[1,9] Ilya Grigoriev,[2] Frederik J.A. van Rijssel,[2] Ruben M. Buey,[1] Aleksandra Lawera,[2] Ilian Jelesarov,[4] Fritz K. Winkler,[1] Kurt Wüthrich,[3,5] Anna Akhmanova,[2,*] and Michel O. Steinmetz[1,*]

[1]Biomolecular Research, Structural Biology, Paul Scherrer Institut, 5232 Villigen PSI, Switzerland
[2]Department of Cell Biology, Erasmus Medical Center, P.O. Box 2040, 3000 CA Rotterdam, The Netherlands
[3]Institute of Molecular Biology and Biophysics, ETH Zurich, 8093 Zurich, Switzerland
[4]Biochemisches Institut der Universität Zürich, Winterthurerstrasse 190, 8057 Zurich, Switzerland
[5]Department of Molecular Biology and Skaggs Institute for Chemical Biology, The Scripps Research Institute, La Jolla, CA 92037, USA
[6]These authors contributed equally to this work
[7]Present address: Novartis Institutes for Biomedical Research, Novartis Pharma AG, 4002 Basel, Switzerland
[8]Present address: Structural and Computational Biology Group, International Centre for Genetic Engineering and Biotechnology (ICGEB), New Delhi 110067, India
[9]Present address: Roche Diagnostics GmbH, 68305 Mannheim, Germany
*Correspondence: a.akhmanova@erasmusmc.nl (A.A.), michel.steinmetz@psi.ch (M.O.S.)
DOI 10.1016/j.cell.2009.04.065

SUMMARY

Microtubules are filamentous polymers essential for cell viability. Microtubule plus-end tracking proteins (+TIPs) associate with growing microtubule plus ends and control microtubule dynamics and interactions with different cellular structures during cell division, migration, and morphogenesis. EB1 and its homologs are highly conserved proteins that play an important role in the targeting of +TIPs to microtubule ends, but the underlying molecular mechanism remains elusive. By using live cell experiments and in vitro reconstitution assays, we demonstrate that a short polypeptide motif, Ser-x-Ile-Pro (SxIP), is used by numerous +TIPs, including the tumor suppressor APC, the transmembrane protein STIM1, and the kinesin MCAK, for localization to microtubule tips in an EB1-dependent manner. Structural and biochemical data reveal the molecular basis of the EB1-SxIP interaction and explain its negative regulation by phosphorylation. Our findings establish a general "microtubule tip localization signal" (MtLS) and delineate a unifying mechanism for this subcellular protein targeting process.

INTRODUCTION

+TIPs constitute a diverse group of evolutionarily conserved microtubule-associated proteins that specifically accumulate at the ends of growing microtubules (Schuyler and Pellman, 2001). They play important roles in essential cellular activities, including chromosome segregation, cell polarization and migration, organelle transport, and intracellular signaling. Furthermore, +TIPs are also implicated in coordinating complex aspects of cell shape and architecture and in the development of cancer (for reviews, see Galjart and Perez, 2003; Carvalho et al., 2003; Akhmanova and Steinmetz, 2008).

+TIPs range in size from a few hundred up to several thousand amino acid residues and consist of multiple domains and/or subunits. End binding protein-1 (EB1) recently emerged as a master regulator of dynamic +TIP interaction networks at growing microtubule ends. Two facts underline its central role. First, EB1 and its family members autonomously track microtubule tips independent of any binding partners, most likely by recognizing structural features of growing microtubule ends (Sandblad et al., 2006; Bieling et al., 2007, 2008; Vitre et al., 2008; Dixit et al., 2009). Second, the C-terminal moiety of EB1 (denoted EB1c) binds to an array of structurally and functionally unrelated +TIP binding partners, including the adenomatous polyposis coli (APC) tumor suppressor protein, the microtubule-actin crosslinking factor (MACF), the cytoplasmic linker protein (CLIP170), CLIP-associated proteins (CLASPs), the transmembrane protein stromal interaction molecule-1 (STIM1), the dynactin large subunit $p150^{glued}$, and the mitotic centromere-associated kinesin (MCAK) (reviewed in Akhmanova and Steinmetz, 2008).

The structure of the C-terminal domain of EB1 has been elucidated by X-ray crystallography (Honnappa et al., 2005; Slep et al., 2005), and a structure-function relationship of its interactions with the cytoskeleton-associated protein-glycine-rich (CAP-Gly) domains of CLIP170 and $p150^{glued}$ has been recently established (Honnappa et al., 2006; Weisbrich et al., 2007; Mishima et al., 2007; Bieling et al., 2008; Dixit et al., 2009; reviewed in Steinmetz and Akhmanova, 2008). However, a general molecular basis of microtubule tip tracking for the majority of EB1-binding partners, which do not contain CAP-Gly domains, remains elusive. A major reason for this lack of knowledge is that prominent +TIPs, such as APC, MACF, CLASPs, STIM1, and MCAK, do not use well-defined, folded domains for EB1 targeting, which makes both functional and

Figure 1. Conservation of the SxIP Motif in Mammalian +TIPs

Sequence alignment of mammalian +TIPs containing basic and serine-rich sequence regions with the SxIP motifs highlighted in orange. Basic and acidic residues are highlighted in blue and red, respectively. Known serine phosphorylation sites in APC and MCAK are underlined and in bold. The dashed line separates proteins where SxIP motif-dependent microtubule tip tracking has been experimentally verified in this work (top sequences) from those that are predicted to be important (bottom sequences). The sequence of the 12-residue MACF2 construct (MACF12LZ), which is sufficient to track microtubule tips as a dimeric GFP-fusion in cells (Figure 2E), is indicated with a bar on top of the alignment. For sequence accession numbers, see Experimental Procedures. Species identifiers are: hs, *Homo sapiens*; mm, *Mus musculus*. The asterisks in MACF2 and p140Cap indicate the C termini of these proteins.

structural studies challenging. Work with APC and MACF suggested that these two proteins both contain an intrinsically unstructured sequence region of approximately 40 residues that binds to EB proteins in vitro (Bu and Su, 2003; Honnappa et al., 2005; Slep et al., 2005). Based on a crystal contact artifact seen in uncomplexed EB1c crystals and mutagenesis, we previously showed that an Ile-Pro dipeptide is important for the interaction of an APC-derived polypeptide fragment with EB1c in vitro (Honnappa et al., 2005). However, it was left open whether these sequence regions and amino acid determinants regulate the microtubule plus-end tracking activity of APC and MACF in cells and, more importantly, whether or not they define a general motif for +TIP interaction with EB1 and for localization to microtubule ends.

Despite the recent progress in understanding EB-dependent microtubule plus-end targeting, many basic questions remain unresolved. (1) Is there a direct correlation between EB1 binding and microtubule plus-end tracking of +TIPs? (2) How is it possible for EB1 proteins to recognize the diverse range of +TIPs in spite of little or no sequence homology among them? (3) What are the sequence requirements and mechanisms that regulate the targeting of +TIPs to EB1 and microtubule ends? By using a multidisciplinary approach, we address these questions in detail in this paper. We establish that the highly conserved C-terminal domain of EB1 recognizes a short linear sequence motif found in a large number of important +TIPs for microtubule plus-end tracking, determine the recognition mechanism in atomic detail, and show how phosphorylation regulates EB1 binding and microtubule tip-targeting activity. Our findings reveal that microtubule plus-end tracking of individual +TIPs in cells can be abrogated by specific mutations in a short sequence stretch, opening the way for detailed analysis of the role of microtubule tip localization in many fundamental cellular activities. On a broader scope, they provide a unifying view of an important subcellular protein targeting process responsible for the dynamic behavior of an array of functionally and structurally diverse proteins.

RESULTS

SxIP Motifs Control Microtubule Plus-End Localization of Diverse +TIPs

To test whether structurally and functionally diverse +TIPs share common sequence motifs, we performed a sequence analysis with the DILIMOT algorithm (see Experimental Procedures). Two related sequence stretches, Ser-x-Ile-Pro-x-Pro and Ser-x-Ile-Pro, were identified as high-significance motif candidates (henceforth termed the SxIP motif, where x denotes any amino acid residue; Figure 1) present within sequence domains that were predicted to be intrinsically disordered. Inspection of the regions flanking the SxIP motif reveals little if any conservation between +TIP families outside of this motif, although high content of serine, proline, and basic residues is evident. This analysis suggests that SxIP motifs embedded within basic and proline/serine-rich sequence regions are characteristic features of +TIPs such as APC, MACF, CLASP, STIM1, and MCAK.

To determine the functional significance of SxIP motifs, we prepared GFP-tagged APC and MACF2 fragments and analyzed their interaction with EB1 by GST pull-down assays and their localization in cells by time-lapse imaging. 39- and 43-residue fragments derived from the C-terminal regions of APC and MACF2 (APC39 and MACF43), respectively, each encompassing one SxIP motif, interacted with EB1 and weakly but significantly tracked growing microtubule ends (Figures 2A, 2B, and 2J; Movies S1 and S2 available online). In order to interfere with EB1 binding and microtubule tip tracking, we replaced the hydrophobic Ile-Pro dipeptide in the SxIP motif of MACF43 (Ile5479 and Pro5480 of human MACF2) with the residues Asn-Asn (MACF43-NN), hypothesizing that if the Ile-Pro dipeptide makes contacts with a hydrophobic surface of EB1, this interaction would be weakened by two polar residues (Honnappa et al., 2005). This residue substitution indeed eliminated binding to EB1 as well as microtubule tip tracking (Figures 2C and 2J; Movie S1). Replacement of the three basic MACF43 residues Lys5478, Arg5484, and Lys5485 within or in the vicinity of the SxIP motif with the polar residues Gln, Asn, and Asn, respectively (MACF43-QNN), also abolished EB1 binding and microtubule end localization (Figures 2D and 2J; Movie S1). Finally, single-site substitutions targeting the serine (replacement with Ala or Asn), isoleucine (Asn), or proline (Asn) residues of SxIP were sufficient to abrogate microtubule tip tracking (Figure S1).

These findings suggest that the identity of the residues at the SxIP motif positions 1, 3, and 4 as well as the presence of basic residues flanking SxIP are important for both binding to EB1 and for tracking of growing microtubule ends in cells.

Multiple SxIP Motifs Act in Concert to Enhance Microtubule Tip Localization

Another well-studied +TIP fragment, CLASP2M, which is derived from the central part of human CLASP2, interacts with EB1 and robustly tracks growing microtubule ends (Figures 2F and 2J; Mimori-Kiyosue et al., 2005). Sequence analysis revealed that human CLASP2 contains two tandemly repeated SxIP motifs within the CLASP2M fragment (Figure 1). To assess the role of these two motifs, we replaced the Ile-Pro dipeptides of the two SxIP motifs individually or simultaneously with the

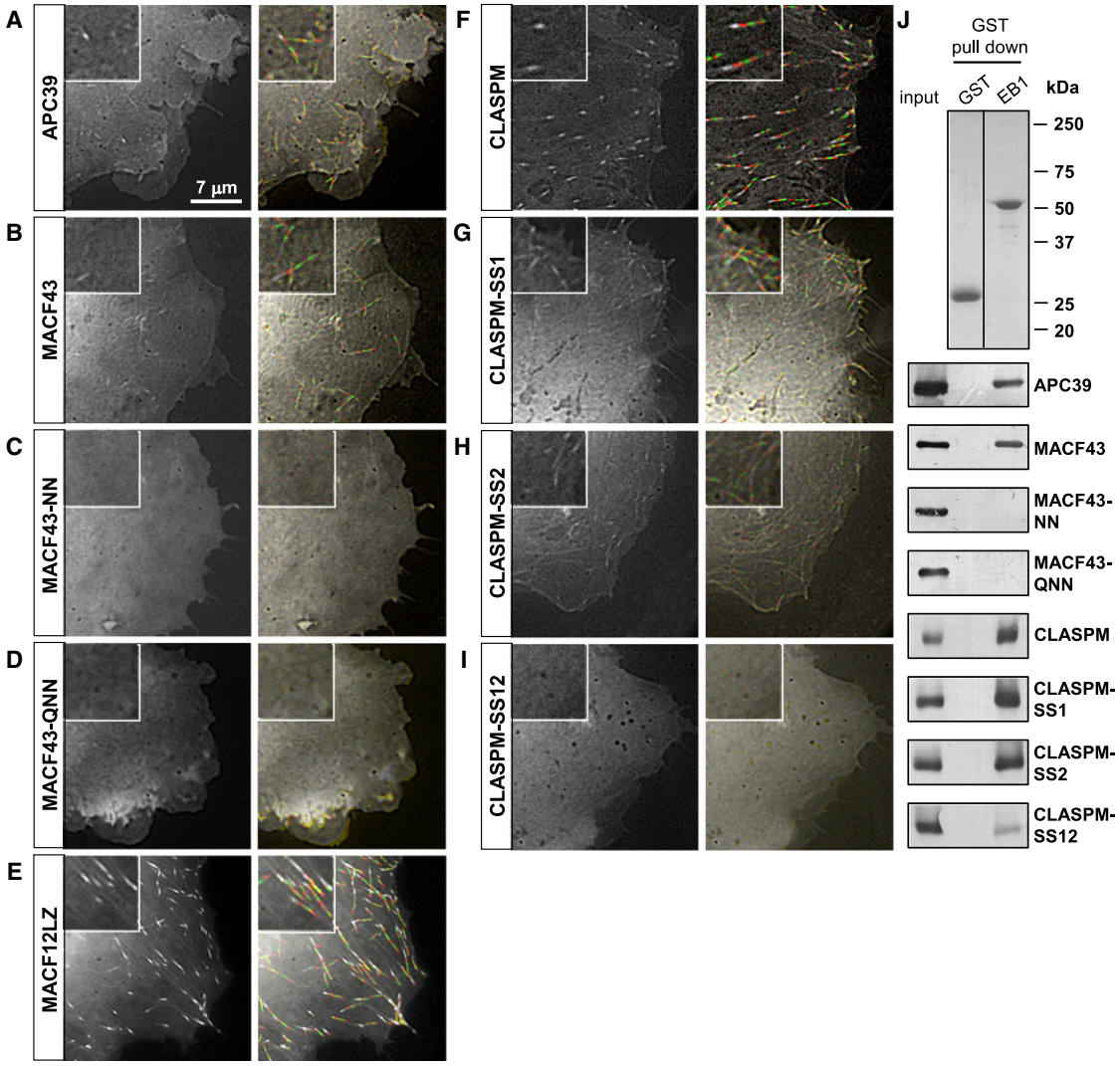

Figure 2. Live Cell Imaging and GST Pull-Down Assays with Wild-Type and Mutant +TIP Fragments

(A–I) Live imaging of cells transiently transfected with the indicated GFP fusions. Left column: frame obtained by averaging of five consecutive images acquired with a 0.5 s interval. Right column: projection of six consecutive averaged frames, covering 2.5 s each. The first frame is shown as grayscale (microtubule plus ends are white), frames 2, 4, and 6 are shown in green (plus ends appear green), and frames 3 and 5 are shown in red (plus ends appear red). This representation facilitates the visualization of moderate microtubule tip tracking events. Insets correspond to enlargements of small parts of the images to illustrate the presence or absence of +TIP localization at growing microtubule ends. COS-7 cells are shown in all images.

(J) GST pull-down assays with GST-EB1 (EB1) or GST alone (GST), with extracts of HEK293 cells expressing the indicated GFP fusions (input). Coomassie staining is shown for the GST proteins and western blots with GFP antibodies for the GFP fusions.

polar dipeptide Ser-Ser (CLASP2M-SS1, CLASP2M-SS2, and CLASP2M-SS12). Introducing Ser-Ser into either of the SxIP motifs of CLASP2M alone did not reduce binding to EB1 in GST pull-down experiments, but it significantly reduced accumulation of the two CLASPM mutants at microtubule tips (Figures 2G, 2H, and 2J; Movie S5). In contrast, CLASP2M-SS12 displayed a strong reduction in EB1 binding and failed to localize to growing microtubule ends (Figures 2I and 2J; Movie S5).

To test the hypothesis that the two SxIP motifs of CLASPM cooperate to enhance microtubule tip tracking, we performed experiments with other +TIP polypeptides. A short 18-residue fragment of MACF43 (MACF18) shows only weak but significant localization to polymerizing microtubule ends (Figure S2; Movie S3). This localization was greatly enhanced by generating a dimeric version of this peptide through N-terminal fusion to the two-stranded leucine zipper (LZ) coiled-coil domain of GCN4 (MACF18LZ; Figure S2; Movie S3). Remarkably, robust plus end tracking was still observed with a dimer of a 12-residue MACF2 peptide (MACF12LZ; Figures 1 and 2E; Movie S4), showing that a surprisingly short polypeptide can mediate microtubule plus-end localization. Dimerization of APC39 (APC39LZ) also resulted in a strong increase in microtubule tip accumulation (Figure S2; Movie S2). These findings show

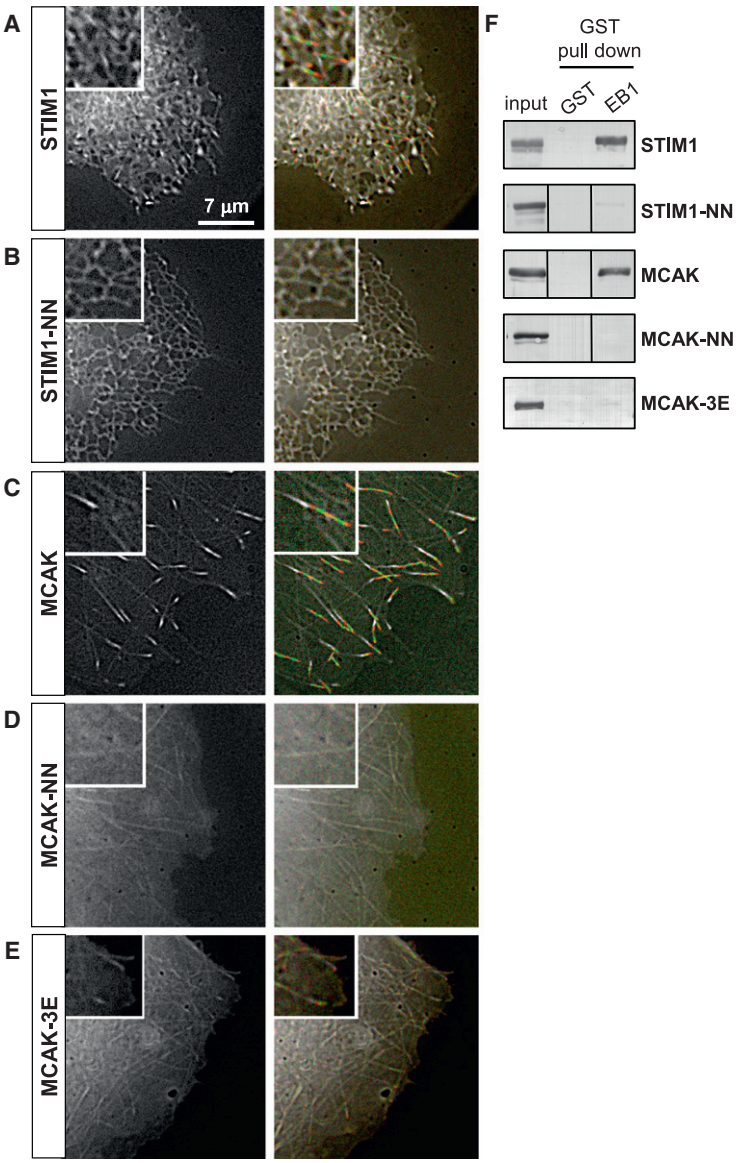

Figure 3. Live Cell Imaging and GST Pull-Down Assays with Wild-Type and Mutant +TIPs

(A–E) Live imaging of cells transiently transfected with the indicated GFP fusions. Images were prepared as described for Figure 2. HeLa and COS-7 cells are shown for the panels with STIM1 and MCAK, respectively.

(F) GST pull-down assays with GST-EB1 or GST alone, using extracts of HEK293 cells expressing the indicated GFP fusions. Black lines separating lanes indicate a composite western blot image; for full blots, see Figure S3.

that concerted action of two SxIP motifs considerably enhances the affinity of +TIPs for growing microtubule plus ends.

Next, we designed experiments with the intention to interfere with the microtubule tip tracking activities of more complex, full-length +TIPs in cells. The first set of experiments was performed with the endoplasmic reticulum (ER) transmembrane protein STIM1. STIM1 contains an N-terminal intra-ER moiety, which is followed by a transmembrane domain and a cytoplasmic C-terminal part that includes an SxIP motif (note that the serine is conservatively replaced by a threonine; Figure 1). Wild-type STIM1 (STIM1-WT) bound EB1 in GST pull-down experiments and tracked microtubule ends at sites where growing microtubule tips contacted the ER membrane network (Figures 3A and 3F; Movie S6; Grigoriev et al., 2008). Replacement of the Ile-Pro dipeptide of the SxIP motif by Asn-Asn (STIM1-NN) abrogated both binding to EB1 and microtubule plus-end tracking (Figures 3B and 3F; Figure S3; Movie S6).

We performed a similar set of experiments with the microtubule-depolymerizing kinesin-13 MCAK. MCAK is a dimer that consists of an N-terminal domain with an SxIP motif (Figure 1), followed by a central motor domain and a C-terminal tail. GFP-tagged wild-type MCAK (MCAK-WT) interacted with EB1, bound the microtubule lattice, and strongly accumulated at polymerizing microtubule ends (Figures 3C and 3F; Figure S3; Movie S7; Moore et al., 2005). In contrast, an MCAK mutant in which the Ile-Pro dipeptide of the SxIP motif was substituted by Asn-Asn (MCAK-NN) displayed no binding to EB1 and no accumulation at microtubule ends, although it could still bind along the microtubule shaft (Figures 3D and 3F; Figure S3; Movie S7). In addition to MCAK, the human kinesin-13 family includes KIF2A and KIF2B, which contain no SxIP motifs within their N termini and are thus predicted not to track microtubule ends. Indeed, both proteins failed to accumulate at polymerizing microtubule ends although they weakly bound microtubule shafts as observed for MCAK-WT and MCAK-NN (Figure S4; Movie S8; Moore et al., 2005).

Taken together, our findings show that a diverse range of +TIPs use SxIP motifs embedded within basic and proline/serine-rich sequence regions to bind to EB1 and to localize to growing microtubule plus ends. Furthermore, tracking of microtubule ends is greatly enhanced by repetition of the SxIP motif within a +TIP or by oligomerization of SxIP motif-containing +TIPs.

Regulation of Microtubule Tip Localization by Phosphorylation

+TIPs are frequently the target of kinases at multiple sites (Akhmanova and Steinmetz, 2008). For example, Ser2789 and Ser2793, which are both in the vicinity of the SxIP motif identified in human APC (Figure 1, underlined), represent Cdc2 and GSK-3β phosphorylation sites, respectively (Nathke, 2004). The effect of phosphorylation at these sites on binding to the C-terminal domain of EB1 (EB1c) was assessed in vitro by isothermal titration calorimetry (ITC) with a polypeptide corresponding to the sequence of APC39 (APCp1; Bu and Su, 2003; Honnappa et al., 2005). ITC revealed that two APCp1 peptides bind to one EB1c dimer, with an equilibrium dissociation constant, K_d,

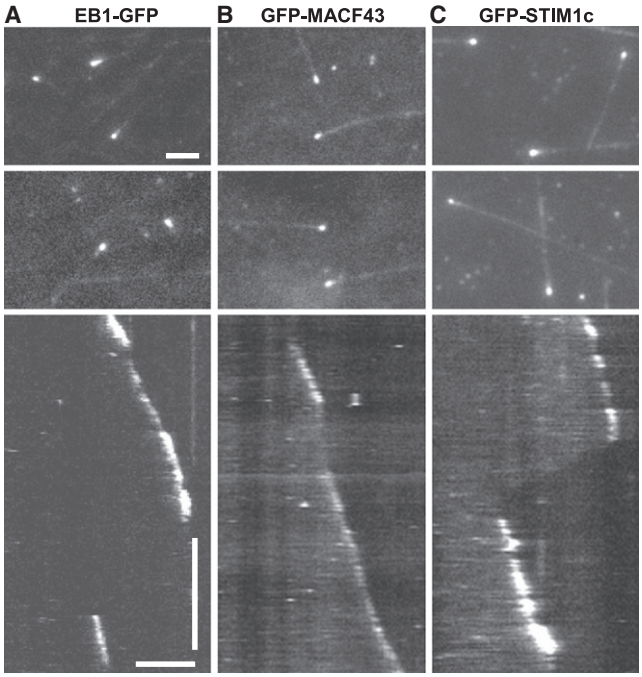

Figure 4. In Vitro Microtubule Tip Tracking

(A) EB1-GFP tracks growing microtubule ends in vitro.

(B and C) GFP-MACF43 (B) and GFP-STIM1c (C) track growing microtubule ends in the presence of unlabeled EB1. Single frames of a TIRFM movie are shown in the upper two panels, and kymographs of individual microtubule ends are displayed in the lower panels. Horizontal bars correspond to 2 μm and the vertical bar to 60 s.

of 5.8 ± 0.1 μM (Figure S5), consistent with previous findings (Honnappa et al., 2005). Peptides phosphorylated at Ser2789 (Honnappa et al., 2005) or Ser2793 (Figure S5) showed ~4- and ~6-fold reduced affinity for EB1c when compared to the wild-type peptide.

The function of MCAK is well known to be regulated by Aurora B phosphorylation (Andrews et al., 2004; Lan et al., 2004). Interestingly, four out of the five Aurora B phosphorylation sites, i.e., Ser95, Ser109, Ser111, and Ser115, cluster in the vicinity of the SxIP motif (Figure 1, underlined). To mimic phosphorylation at these sites, we simultaneously mutated three of these serine residues, Ser95, Ser109, and Ser111, to glutamate (MCAK-3E). In cells, the phosphomimicking MCAK mutant accumulated along microtubules in a manner that was similar to the wild-type protein. In contrast to the wild-type protein, however, MCAK-3E bound only very weakly to EB1 in GST pull-down experiments and failed to track growing microtubule ends (Figures 3E and 3F; Movie S7). This finding is in agreement with a previous study showing that mutating all five Aurora B phosphorylation sites to glutamates abolishes microtubule tip tracking (Moore et al., 2005).

A recent study suggested that GSK3β-mediated phosphorylation of several serine residues surrounding the SxIP sites of CLASP2 interferes with the binding to EB1 and to microtubule tips (Kumar et al., 2009). Overall, these data demonstrate that phosphorylation in the vicinity of SxIP motifs negatively regulates the localization of +TIPs to microtubule ends by decreasing their affinity for EB1.

In Vitro Reconstitution of EB1-Dependent Microtubule Tip Tracking

To test whether EB1 is sufficient for localizing proteins containing SxIP motifs to growing microtubule ends, we reconstituted the process with purified components (Bieling et al., 2007). GFP-labeled human EB1-tracked growing microtubule ends as previously described (Figure 4A; Movie S9; Bieling et al., 2007, 2008; Dixit et al., 2009). In the presence of unlabeled EB1, both GFP-tagged MACF43 and a 436-residue C-terminal fragment of STIM1 encompassing the SxIP motif (STIM1c; Grigoriev et al., 2008) weakly labeled the microtubule lattice and strongly accumulated at growing microtubule ends (Figures 4B and 4C; Movies S10 and S11). In the absence of EB1, however, we observed only microtubule lattice binding but no tip localization of MACF43 and STIM1c (Figure S6).

Given that modification of the SxIP motif within +TIPs has been shown to interfere with their localization to growing microtubule tips in cells (Figures 2 and 3), these in vitro results imply that the EB1-SxIP motif interaction is not only necessary but also sufficient for many +TIPs to track growing microtubule ends.

Structural Analysis of the EB1-SxIP Binding Mode

To obtain insight into the structural basis of SxIP motif recognition by EB1, we attempted to crystallize a complex formed between EB1c and a representative peptide from one of the +TIPs. After screening of different constructs, we succeeded in solving the structure of an EB1c fragment lacking the last 8 C-terminal residues (EB1cΔC8) in a complex with a 30-residue peptide derived from the C-terminal region of human MACF2 (MACFp1; residues 5468–5497) at 2.5 Å resolution by X-ray crystallography (Table 1; Figure 5).

The previously determined crystal structure of the uncomplexed EB1c dimer showed a parallel 2-stranded coiled coil followed by the EBH domain containing a 4-helix bundle and a disordered C-terminal tail (Honnappa et al., 2005; Slep et al., 2005). Highly conserved structural features on the surface of the EB homology (EBH) domain are a hydrophobic cavity, anticipated to bind nonpolar residues from interaction partners (Honnappa et al., 2005), and an adjacent polar rim. In the EB1cΔC8-MACFp1 complex, two EB1cΔC8 dimers are present in the asymmetric unit. Well-defined electron density was observed for MACFp1 in three of the four crystallographically independent binding sites. The ordered segments differ in length (8, 9, and 11 residues), but they all include the heptapeptide Pro5476-Ser-Lys-Ile-Pro-Thr-Pro bound in very similar conformations. Residues outside this core segment are less well defined and do not participate in specific intermolecular interactions. Residues 250–257 of EB1c, which are not resolved in the crystal structure of the uncomplexed EB1c dimer (Honnappa et al., 2005; Slep et al., 2005), have become structured in the EB1cΔC8-MACFp1 complex and form a handle-shaped loop wrapped around the bound peptide (Figures 5A–5C). The common heptapeptide segment is in slightly bent conformation and interacts with EB1cΔC8 through both main chain and side chain atoms (Figure 5C).

Table 1. X-Ray Data Collection and Refinement Statistics

	EB1cΔC8-MACFp1
Wavelength, Å	1.0009
Space group (no.)	$P2_1$ (4)
Resolution range, Å	50-2.5 (2.56-2.5)
Unit cell, *a*, *b*, and *c* in Å	45.6, 44.9, 74.8, β = 98.6°
No. of observed reflections	31520
No. of unique reflections	10167
R_{sym}[b], %	8.8 (42.6)[a]
I/σ (*I*)	9.9 (3.4)[a]
Completeness, %	96.1 (97.6)[a]
No. of Refined Atoms	
Proteins/peptides	2290
Water	19
R-factor/free *R*-factor[c]	0.22/0.25
Rmsd bond lengths/bond angles[d]	0.01/1.1

[a] Figures in parentheses indicate the values for the outer shell of the data.
[b] $R_{sym} = \sum_h\sum_i | I_i(h) - <I(h)> | / \sum_h\sum_i I_i(h)$, where $I_i(h)$ and $<I(h)>$ are the *i*th and mean measurement of the intensity of reflection *h*.
[c] $R = \sum|F_P^{obs} - F_P^{calc}|/ \sum F_P^{obs}$, where F_P^{obs} and F_P^{calc} are the observed and calculated structure factor amplitudes, respectively.
[d] Rmsd, root-mean-square-deviation from the parameter set for ideal stereochemistry.

The most prominent contacts involve Ser5477, Ile5479, and Pro5480, which occupy the positions 1, 3, and 4 of the SxIP motif from MACFp1. Ser5477 forms an extensive network of hydrogen bonds with the highly conserved Arg222, Glu225, Gln229, and Tyr247 residues of EB1cΔC8 and a water molecule (Figures 5C and 5D). The dipeptide Ile5479-Pro5480 of MACFp1 is deeply buried within a cleft of EB1cΔC8 shaped by the residues Phe216-Arg222, Glu225, Leu241, and Tyr247 of the hydrophobic cavity and the residues Ala248-Pro256 of the C-terminal tail region. Lys5478, the x residue of the SxIP motif, is within salt bridging distance to Asp257 of EB1cΔC8; however, only poorly defined electron density is seen for both side chains, indicating conformational flexibility. Further contacts are observed between Thr5481 and Pro5482 of MACFp1, and Glu213, Phe253, Gly252, and Val254 of EB1cΔC8.

In order to determine whether the structural features observed in the EB1cΔC8-MACFp1 complex apply more generally to EB1-mediated +TIP interactions, we performed nuclear magnetic resonance (NMR) experiments on the EB1c-APCp1 complex. $^{15}N\{^1H\}$-NOEs demonstrate that whereas APCp1 is unstructured in solution (not shown), the segment 2784–2813 is ordered in the complex with EB1c (Figure 6A). Chemical shift changes and intermolecular ^1H-^1H NOEs identify residues 2803–2809 encompassing the SxIP motif as a major interaction site, with secondary interactions at residues 2789–2799 (Figure 6A; Figure S7). The remainder of the APCp1 polypeptide is disordered even in the bound state. In free EB1c, the polypeptide segment 194–250 is predominantly structured in solution, whereas the segment 252–268 appears to be flexibly disordered. In complex with APCp1, residues 250–257 of EB1c become ordered (Figure 6B), and chemical shift changes indicate that these residues together with residues 213–225 and 247–249 of the hydrophobic cavity and the polar rim are the major interaction sites (Figure 6C; Figure S7). Deletion of the C-terminal 20-residue segment of EB1c (EB1cΔtail) abrogates binding to APCp1 (Figure S5), consistent with its important role for complex formation. Overall, the NMR studies indicate a rather dynamic EB1c-APCp1 interaction in solution, which compliments the observation of micromolar complex stability by ITC (Figure S5).

The interactions observed in the X-ray crystal structure of the EB1cΔC8-MACFp1 complex are in agreement with all data obtained by NMR, indicating that the structures of the two complexes are very similar.

DISCUSSION

It is well established that the many central activities of +TIPs in cells are tightly associated with their common property to track growing microtubule ends. By combining structural and biophysical data with in vitro reconstitution and cell biological approaches, we here provide detailed mechanistic information on the phenomenon of microtubule tip tracking. We establish that a short, conserved, and phosphorylation-controllable motif, SxIP, within basic and proline/serine-rich sequence domains, targets a number of functionally and structurally unrelated +TIPs to growing microtubule ends in an EB1-dependent manner. Our findings thus provide molecular insights into the master role of EBs in integrating diverse binding partners within dynamic +TIP networks.

Our structural data demonstrate that EBH domains are SxIP motif recognition domains. This conclusion is supported by the finding that all EB1c residues that interact with the SxIP motifs in the two complexes studied at atomic detail, EB1cΔC8-MACFp1 and EB1c-APCp1, are located within the EBH domain and are highly conserved from yeast to humans, suggesting a strong functional selection. A key feature of the EBH-SxIP binding mode is the interaction network established between the serine, isoleucine, and proline residues at motif positions 1, 3, and 4 and the hydrophobic cleft of the EBH domain. Based on modeling, we expect that some conservative substitutions for these three key residues might be tolerated as seen, for example, in STIM1 and p140Cap where the serine at motif position 1 is conservatively replaced by threonine (Figure 1). However, replacement of this position 1 serine by the residues asparagine or alanine interferes with the formation of the hydrogen bonding network mediated by the serine side chain, and this modification did in fact abrogate microtubule tip tracking by MACF43. Similarly, mutating the apolar isoleucine and proline at motif positions 3 and 4 either individually or simultaneously to polar residues (asparagines or serines) disrupts their packing interactions with the hydrophobic cleft of EBH and abrogates binding to EB1 and tracking of microtubule ends of a diverse set of +TIPs in cells. Mutations targeting the EBH domains also impact the EBH-SxIP interaction: deletion of the C-terminal tail region of EB1c abolishes binding to APCp1, because the segment 247–257 of EBH makes extensive contacts to SxIP in the complex. Similarly, mutations affecting the hydrophobic cavity or the polar rim of EB1c weakened or abrogated binding to a polypeptide fragment derived from the

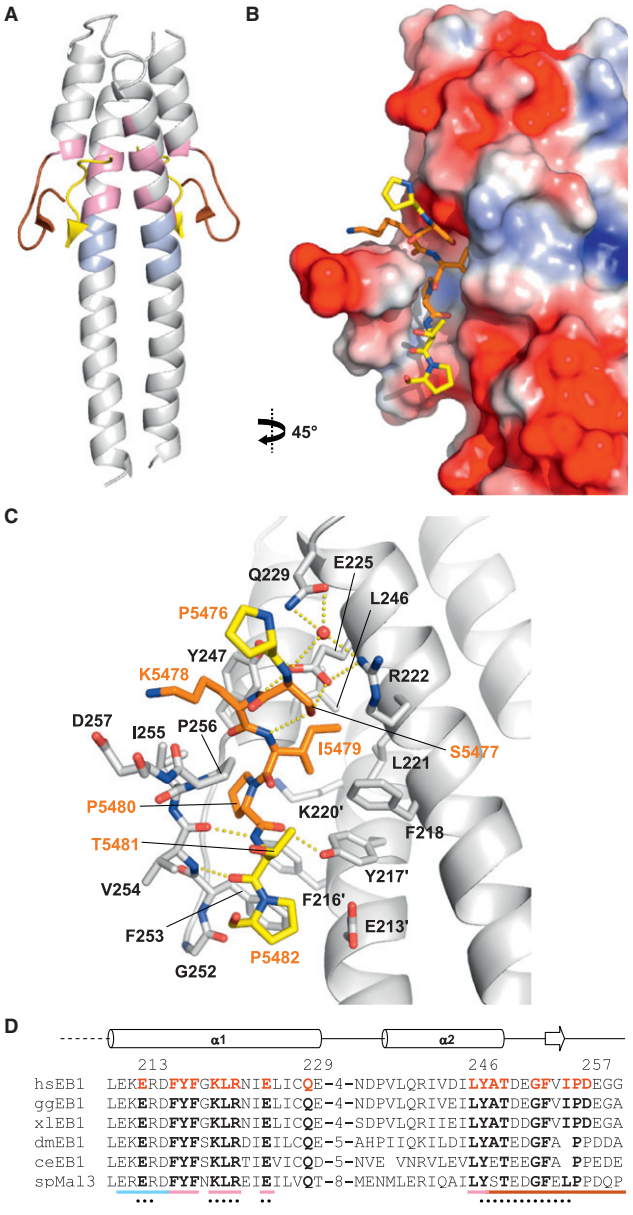

Figure 5. X-Ray Crystal Structure of the EB1cΔC8-MACFp1 Complex

(A) Cartoon of the ternary complex formed between EB1cΔ8 (light gray) and MACFp1 (yellow). Residues originating from the hydrophobic cavity, the polar rim, and the C-terminal tail region of the EBH domain of EB1cΔ8 are highlighted in pink, light blue, and brown, respectively.

(B) Surface view of EB1cΔ8 color-coded with the electrostatic potential (from −15 to +15 k_BT; red and blue depict negative and positive electrostatic potentials, respectively) and a stick representation of MACFp1.

(C) Close-up view of the interaction network seen in the EB1cΔ8-MACFp1 complex. An ordered water molecule is represented as a small red sphere. Hydrogen bonds are depicted by dashed yellow lines. The carbon atoms of MACFp1 outside of the SxIP motif are colored in yellow, those within the SxIP motif (Ser5477-Lys-Ile-Pro) in orange; in the stick representation of MACFp1, the oxygen and nitrogen atoms are colored red and blue, respectively.

(D) Sequence alignment of EBH domains. Residues making intermolecular contacts in the EB1cΔ8-MACFp1 complex structure are highlighted in red. Conserved residues making intermolecular contacts in the complex are indicated in bold. Secondary structure elements and human EB1 residue numbering are indicated on top of the alignment. EBH amino acids engaged in interactions with MACFp1 are grouped into three polypeptide segments, which are identified with light blue, pink, and brown bars beneath the alignment to indicate their location in the polar rim, the hydrophobic cavity, and the C-terminal tail region of EBH domains, respectively (see also A). Dotted lines identify residues with sizeable chemical shift changes upon binding to APCp1 (Figure S7). Species identifiers are as follows: hs, *Homo sapiens*; gg, *Gallus gallus*; xl, *Xenopus laevis*; dm, *Drosophila melanogaster*; ce, *Caenorhabditis elegans*; and sp, *Saccharomyces pombe*.

C-terminal part of APC (Wen et al., 2004). Overall, these findings underscore the functional relevance of the EBH-SxIP interaction.

The structure of the complex formed between EBH and SxIP is very different from those formed between the CAP-Gly domains of CLIP170 and $p150^{glued}$ and the C-terminal domain of EB1. Although linear SxIP motifs within +TIPs target the hydrophobic cavity and the N-terminal portion of the EB1c C-terminal tail, the globular CAP-Gly domains specifically recognize the EEY/F motif at the very C terminus of EB1c (Honnappa et al., 2006; Weisbrich et al., 2007; Mishima et al., 2007). This difference in binding mechanism explains why the addition of tags, such as GFP, to the C termini of EBs strongly interferes with EB binding to CAP-Gly proteins, but not to SxIP motif-containing +TIP partners (Komarova et al., 2005; Mimori-Kiyosue et al., 2005; Weisbrich et al., 2007). Notably, residues 247–257 of the C-terminal tail from EB1, which make important interactions with the SxIP motif of +TIPs, are separated by eight residues from the C-terminal EEY/F motif that targets CAP-Gly domains. This close juxtaposition suggests that the two interactions may either cooperate or interfere with each other and in this way couple the functioning of these two recognition motifs.

Inspection of the sequences flanking SxIP motifs reveals an enrichment of proline, serine, and basic residues, which cause locally reduced flexibility (assessed for APCp1 by NMR; data not shown) and lead to a net positive charge of the polypeptide segments. The basic residues are anticipated to mediate long-range attractive electrostatic interactions between the negatively charged patches of the EBH surface and the acidic residues of the flexible C-terminal tail of EB1. Several such electrostatic interactions occur at the EB1cΔC8-MACFp1 interface: Lys5478, Lys5475, and Lys5485 of MACFp1 are within salt bridge distance (<6 Å) of Asp257, Glu232, and Asp209 from EB1cΔC8, respectively (not shown). These observations explain why phosphorylation of serine residues in the vicinity of the SxIP motif negatively regulates the localization of +TIPs to microtubule ends: introduction of negative charges is expected to reduce the long-range attractive electrostatic interactions contributing to the stability of the complex between EBH domains and SxIP-containing polypeptide segments.

The affinity of individual +TIP-EB1 interactions is rather weak (low micromolar range). However, our data demonstrate that multiple SxIP motifs, either within the same polypeptide chain or within different polypeptide chains, cooperate to increase the EB-dependent targeting efficiency. Because +TIPs are frequently multidomain and/or multisubunit proteins, we expect that many +TIPs may use more than one SxIP motif to robustly track growing microtubule ends. The additive nature of these

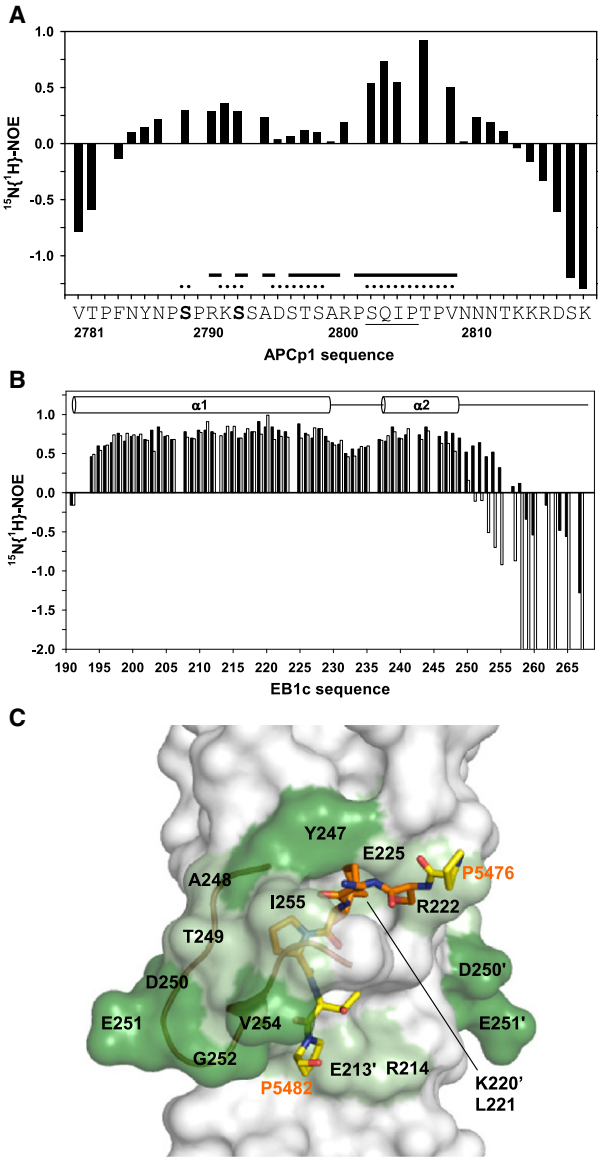

Figure 6. Solution NMR Analysis of the EB1c-APCp1 Complex

(A) $^{15}N\{^{1}H\}$-NOE values of uniformly ^{15}N-labeled APCp1 in complex with unlabeled EB1c. At the bottom, dotted lines identify polypeptide segments with sizeable chemical shifts changes upon binding to EB1c, and solid lines those with intermolecular ^{1}H-^{1}H NOEs to EB1c (Figure S7). Free APCp1 showed random coil ^{1}H chemical shifts (Figure S7) and negative $^{15}N\{^{1}H\}$-NOEs for all the residues (not shown), which is typical for a predominantly extended disordered polypeptide. After binding to EB1c, the segment 2785–2813 becomes ordered, showing positive $^{15}N\{^{1}H\}$-NOEs that indicate motional restriction, while the remainder of the polypeptide remains disordered even in the bound state. Chemical shift changes upon binding are seen for the backbone amide groups of residues 2789–2799 and 2803–2809, which also have positive $^{15}N\{^{1}H\}$-NOEs and intermolecular ^{1}H-^{1}H NOEs to hydrogen atoms in EB1c. High density of such NOEs suggests that the segment 2803–2807 makes the tightest contacts with EB1c. The Ser2789 and Ser2793 phosphorylation sites are indicated in bold. The SxIP motif is underlined.

(B) $^{15}N\{^{1}H\}$-NOE values of uniformly ^{15}N-labeled EB1c free (white bars) and in complex with unlabeled APCp1 (black bars). The residues 194–250 have positive $^{15}N\{^{1}H\}$-NOE values, which indicates that the structured state of this polypeptide segment observed in the crystal structure of free EB1c (Honnappa et al., 2005; Slep et al., 2005) is preserved in solution. The segment 252–268 is disordered in free EB1c but in complex with APCp1, the positive $^{15}N\{^{1}H\}$-NOEs of residues 250–257 show that this polypeptide segment is in a motionally constrained state.

(C) Combined chemical shift changes of backbone ^{15}N and H^{N} resonances from EB1c because of complex formation with APCp1 are indicated on a semi-transparent surface representation of complexed EB1cΔ8 (Figure 5), with values larger than one or two standard deviations from the mean chemical shift change for the data set (Figure S7) colored in light and dark green, respectively. The C-terminal tail sequence of EB1c is shown in a brown stick cartoon representation. The carbon atoms of MACFp1 outside of the SxIP motif are colored in yellow, those within the SxIP motif (Ser5477-Lys-Ile-Pro) in orange. In the stick representations, oxygen and nitrogen atoms are colored red and blue, respectively.

interactions means that localization of +TIPs to microtubule ends can be precisely regulated by reducing the affinity of +TIPs through phosphorylation of individual SxIP sites. Furthermore, moderately stable but specific interactions involving diverse multidomain and/or multisubunit proteins are well suited to control highly dynamic and complex cellular processes where contacts need to be continuously broken and reformed in response to spatial movement of the target structure, such as a growing microtubule plus end.

EB proteins autonomously track microtubule tips most likely by recognizing a structural feature of the growing microtubule end via their N-terminal domain (Sandblad et al., 2006; Bieling et al., 2007; Vitre et al., 2008; Komarova et al., 2009). Because of the evolutionary conservation of this domain from yeast to humans, it is expected that the vast majority of growing microtubules in eukaryotic cells carry EBs at their tips (Mimori-Kiyosue et al., 2000; Busch and Brunner, 2004). Our data thus suggest that the SxIP motif acts as a general microtubule tip localization signal (MtLS) that targets structurally and functionally diverse +TIPs to microtubule ends by binding to EBs. The possibility to identify MtLSs and to rationally interfere with their function by introducing amino acid substitutions within a very short sequence stretch will now enable systematic dissection of the role of EB association and microtubule tip tracking in fundamental cellular processes.

EXPERIMENTAL PROCEDURES

Protein and Peptide Preparations

The insertion of full-length human EB1, EB1c (Asp191-Tyr268) and EB1cΔtail (Asp191-Ala248) into a pET15b (Invitrogen) derivative has been described (Honnappa et al., 2005, 2006). EB1cΔC8 (Asp191-Gly260) in the same vector was obtained by PCR amplification from the EB1c clone. APCp1 (Val2781-Lys2819 of human APC) and MACFp1 (Gly5468-Arg5497 of human MACF2) were cloned with synthetic DNA oligonucleotides into a pET15b derivative encoding for an N-terminal 6xHis tag followed by thioredoxin and a thrombin cleavage site. GFP-STIM1c (Gly250-Lys685 of human STIM1) and GFP-MACF43 (MACFp1 extended by six N-terminal residues) with an N-terminal 6xHis tag were cloned in pET28a. EB1-GFP with a C-terminal 6xHis tag was also cloned in pET28a.

Recombinant protein expression and purification have been performed as described (Honnappa et al., 2005, 2006; Weisbrich et al., 2007). For the preparation of ^{15}N- and ^{13}C,^{15}N-uniformly labeled protein and peptide samples, cells were grown in a minimal medium (Honnappa et al., 2003). Affinity purification of the N-terminal 6xHis-tagged fusion proteins by immobilized metal affinity chromatography on Ni^{2+}-Sepharose (Amersham) was performed at 4°C according to the manufacturer's instructions. The 6xHis fusion-tag was

removed from recombinant proteins and peptides by thrombin (Sigma) cleavage. Protein and peptide samples were gel filtered on a Superdex-75 column (Amersham) equilibrated in 20 mM Tris-HCl (pH 7.5), supplemented with 75 mM NaCl. Recombinant EB1c and APCp1 samples for NMR experiments were further purified by HPLC on a C18 reverse phase column and lyophilized.

N-acetylated and C-amidated APCp1 and APCp1-pSer2793 peptides were assembled on an automated continuous-flow synthesizer employing standard methods.

The homogeneity of the recombinant proteins and peptides were confirmed by either 15% SDS-PAGE, Tricine-SDS-PAGE, or HPLC and their identities were assessed by mass spectral analyses. Exact concentrations of protein and peptide solutions were determined by tyrosine and tryptophan absorbance at 276 nm in 6 M GuHCl except for the NMR samples where the concentrations for APCp1 was determined via the PULCON method (Wider and Dreier, 2006).

GST Pull-Down Assays

Purification of GST fusions and GST pull-down assays with extracts of HEK293 cells transiently expressing various GFP-tagged proteins was performed as described previously (Grigoriev et al., 2008). All pull downs were performed in the presence of 150 mM NaCl, with the exception of MCAK and CLASP2M pull downs that were performed in the presence of 300 mM NaCl.

Nuclear Magnetic Resonance

All NMR experiments were performed at 45°C with 1 mM protein solutions (5 mM sodium phosphate buffer at pH 6.5 containing Roche protease inhibitor EDTA-free [1 tab per 100 ml] and 0.2 mM phenylmethylsulfonylflouride).

Bruker Avance 900, DRX 750, and DRX 500 spectrometers were used. Sequence-specific backbone resonance assignments were obtained with HNCA, HNCACB, CBCA(CO)NH, HNCO, and HN(CA)CO triple resonance experiments and ^{15}N-resolved [^{1}H,^{1}H]-NOESY spectra. Side-chain assignments of APCp1 were obtained with (H)C(CCCO)NH, H(CCCO)NH, and HC(C)H-TOCSY spectra (Cavanagh et al., 1996). Intermolecular ^{1}H–^{1}H NOEs between APCp1 and EB1c were identified by comparison of a 3D ^{13}C(ω_1)-filtered,^{13}C(ω_2)-resolved [^{1}H,^{1}H]-NOESY spectrum with a 3D ^{13}C(ω_1)-selected,^{13}C(ω_2)-resolved [^{1}H,^{1}H]-NOESY spectrum (Zwahlen et al., 1997) recorded with a complex of uniformly ^{13}C,^{15}N-labeled APCp1 with unlabeled EB1c in $^{2}H_2O$ solution. NOESY spectra were measured at 900 MHz with a mixing time of 60 ms or at 750 MHz with a mixing time of 100 ms. Steady-state ^{15}N{^{1}H}-NOEs were measured at 500 MHz with a saturation period of 4 s (Dayie and Wagner, 1994). The program CARA (http://www.nmr.ch) was used for the analysis of NMR spectra (Keller, 2004). Combined chemical shift changes were calculated by taking the square root of the sum of the squares of the chemical shift changes for the backbone $^{1}H^{N}$ and ^{15}N resonances after scaling the ^{15}N shifts by 0.15.

Isothermal Titration Calorimetry

ITC experiments were performed at 25°C as described (Honnappa et al., 2005). The sample cell and syringe were filled with ~100 μM EB1c protein (monomer equivalents) and ~1 mM APCp1 or MACFp1 peptide solutions, respectively. The protein and peptide samples had been extensively dialyzed against 10 mM sodium phosphate buffer (pH 7.4) supplemented with 150 mM NaCl prior to the experiment. The binding isotherms were fitted by a nonlinear least-squares minimization method provided with the VP-ITC calorimeter (Microcal Inc., Northampton, MA).

X-Ray Crystallography

EB1c (1 mM monomer concentration) was cocrystallized with MACFp1 (1 mM) via the sitting drop method at 20°C by mixing equal volumes of the protein/peptide solutions. Crystals were grown with a reservoir solution containing 200 mM magnesium acetate and 20% PEG 3350. Synchrotron data sets were collected at the Swiss Light Source (Villigen PSI, Switzerland) protein beam line X06SA on a pixel-counting PILATUS 6M detector. X-ray diffraction data were collected at 100 K. The EB1c-MACFp1 complex structure was solved by molecular replacement with the structure of EB1c (PDB ID code 1WU9) as a search model. Data collection and refinement statistics are given in Table 1.

Figures displaying structures were prepared with the program PyMOL (DeLano Scientific LLC, San Carlos, CA, http://www.pymol.org). Electrostatic calculations were performed in PyMOL with the APBS plug-in (Baker et al., 2001).

Sequence Analysis with DILIMOT

DILIMOT (version 2006; Neduva et al., 2005) analysis was performed with the following +TIPs that contain basic and serine-rich sequence regions and which were experimentally verified to bind to EB proteins (see Akhmanova and Steinmetz, 2008, and references therein or indicated references; sequence accession numbers are indicated in parentheses): APC (P25054), MACF2 (NP_899236), CLASP2 (O75122), STIM1 (Q13586), MCAK (Q99661), DDA3 (NP_064360), melanophilin (Q91V27), CLIP170 (P30622), p150^{glued} (Q14203), p140Cap (Q75T46; Jaworski et al., 2009), XMAP215 (Q9PT63), RhoGEF2 (A1ZAN6). The sequences were automatically filtered for globular domains, signal peptides, trans-membrane, and coiled-coil regions prior to analysis.

Mammalian Expression Constructs and Plasmid Transfection

N-terminal GFP-tagged human STIM1, KIF2A, and KIF2B were generous gifts of R. Lewis (Stanford University, Stanford, CA), D. Compton (Dartmouth Medical School, Hanover, NH), and L. Wordeman (University of Washington, Seattle, WA), respectively. Human MCAK was cloned by PCR from the MegaMan cDNA library (Stratagene) into the Gateway entry vector pDONR221 (Invitrogen). GFP fusions of various MCAK, MACF2, APC, CLASP2, and STIM1 constructs were generated in pEGFP-C2 (Clontech) or in pcDNATM6.2/N-EmGFP-DEST (Invitrogen) via PCR-based strategies or the Gateway cloning system, respectively. Mutagenesis was carried out with the Quick Change kit (Stratagene). The two-stranded leucine zipper coiled-coil sequence corresponding to GCN4-p1 (Steinmetz et al., 2007) was fused to the N termini of MACF2 and APC peptides by a PCR-based strategy. Plasmids were transiently transfected in COS-7 or HeLa cells via Polyfect (QIAGEN).

Residue boundaries of +TIP fragments are as follows (for accession numbers, see above): APC39, Val2781-Lys2819 of human APC; MACF43, Glu5455-Arg5497 of human MACF2; MACF18, Gly5468-Lys5485; MACF12, Ala5474-Lys5485; CLASP2M, Arg444-Ser580 of human CLASP2.

In Vitro Microtubule End-Tracking Assay and Live Cell Imaging

The microtubule end-tracking assay was performed as previously described (Komarova et al., 2009). The concentration of EB1-GFP was 20 nM; the final concentrations of GFP-MACF43 and GFP-STIM1c (residues 250–685 of human STIM1) for the experiments presented in Figure 4 were 12.5 nM each together with 200 nM and 50 nM of unlabelled EB1, respectively.

Total internal reflection fluorescence microscopy (TIRFM) and wide-field time-lapse imaging was performed on an inverted research Nikon Eclipse TE2000E (Nikon) microscope with a CFI Apo TIRF 100×1.49 N.A. oil objective (Nikon). The microscope was equipped with a QuantEM EMCCD camera (Roper Scientific) and was controlled by the MetaMorph 7.1 software package (Molecular Devices). For excitation, we used HBO 103 W/2 Mercury Short Arc Lamp (Osram) and Chroma ET-GFP filter cube for wide-field imaging and 113 mW, 488 nm line of an argon laser (Spectra-Physics Lasers) and Chroma ET-GFP filter cube for TIRFM. 16-bit images were projected onto the CCD chip at a magnification of 0.067 μm/pixel. Analysis and averaging of images was performed with MetaMorph; further image processing, including adjustment of levels, application of Unsharp mask, and Gaussian Blur Filter were carried out with Adobe Photoshop. For live cell imaging of each construct, at least five transfected cells expressing low levels of the GFP fusion were imaged and a representative image was selected. None of the analyzed constructs had a significant effect on the number or the staining intensity of the EB1-positive microtubule ends at low expression levels (data not shown).

ACCESSION NUMBERS

Coordinates of the EB1cΔC8-MACFp1 complex structure has been deposited with accession code 3GJO in the Protein Data Bank.

SUPPLEMENTAL DATA

Supplemental Data include 7 figures and 11 movies and can be found with this article online at http://www.cell.com/cell/supplemental/S0092-8674(09)00638-2.

ACKNOWLEDGMENTS

We are indebted to A. Blanc, D. Desbouis, and C. Müller for excellent technical assistance, to N. Olieric for cloning of human MCAK, to A. Mussachio for critical reading and comments on the manuscript, and to R. Lewis, D. Compton, and L. Wordeman for the generous gift of materials. X-ray data were collected at beamline X06SA of the Swiss Light Source (Paul Scherrer Institut, Villigen, Switzerland). This work was supported by the Swiss National Science Foundation (to M.O.S.), by the Netherlands Organization for Scientific Research (to A.A.), by Fundação para a Ciência e a Tecnologia fellowship (to S.M.G.), by a FEBS fellowship to R.M.B., and by the Swiss National Science Foundation and the ETH Zürich through the NCCR "Structural Biology" (to I.J., F.K.W., and K.W.).

Received: November 10, 2008
Revised: March 9, 2009
Accepted: April 27, 2009
Published: July 23, 2009

REFERENCES

Akhmanova, A., and Steinmetz, M.O. (2008). Tracking the ends: a dynamic protein network controls the fate of microtubule tips. Nat. Rev. Mol. Cell Biol. *9*, 309–322.

Andrews, P.D., Ovechkina, Y., Morrice, N., Wagenbach, M., Duncan, K., Wordeman, L., and Swedlow, J.R. (2004). Aurora B regulates MCAK at the mitotic centromere. Dev. Cell *6*, 253–268.

Baker, N.A., Sept, D., Joseph, S., Holst, M.J., and McCammon, J.A. (2001). Electrostatics of nanosystems: application to microtubules and the ribosome. Proc. Natl. Acad. Sci. USA *98*, 10037–10041.

Bieling, P., Laan, L., Schek, H., Munteanu, E.L., Sandblad, L., Dogterom, M., Brunner, D., and Surrey, T. (2007). Reconstitution of a microtubule plus-end tracking system in vitro. Nature *450*, 1100–1105.

Bieling, P., Kandels-Lewis, S., Telley, I.A., van Dijk, J., Janke, C., and Surrey, T. (2008). CLIP-170 tracks growing microtubule ends by dynamically recognizing composite EB1/tubulin-binding sites. J. Cell Biol. *183*, 1223–1233.

Bu, W., and Su, L.K. (2003). Characterization of functional domains of human EB1 family proteins. J. Biol. Chem. *278*, 49721–49731.

Busch, K.E., and Brunner, D. (2004). The microtubule plus end-tracking proteins mal3p and tip1p cooperate for cell-end targeting of interphase microtubules. Curr. Biol. *14*, 548–559.

Carvalho, P., Tirnauer, J.S., and Pellman, D. (2003). Surfing on microtubule ends. Trends Cell Biol. *13*, 229–237.

Cavanagh, J., Fairbrother, W.J., Palmer, A.G., and Skelton, N.J. (1996). Protein NMR Spectroscopy: Principles and Practice (London: Academic Press).

Dayie, K.T., and Wagner, G. (1994). Relaxation-rate measurements for ^{15}N-^{1}H groups with pulsed-field gradients and preservation of coherence pathways. J. Magn. Reson. A *111*, 121–126.

Dixit, R., Barnett, B., Lazarus, J.E., Tokito, M., Goldman, Y.E., and Holzbaur, E.L. (2009). Microtubule plus-end tracking by CLIP-170 requires EB1. Proc. Natl. Acad. Sci. USA *106*, 492–497.

Galjart, N., and Perez, F. (2003). A plus-end raft to control microtubule dynamics and function. Curr. Opin. Cell Biol. *15*, 48–53.

Grigoriev, I., Gouveia, S.M., van der Vaart, B., Demmers, J., Smyth, J.T., Honnappa, S., Splinter, D., Steinmetz, M.O., Putney, J.W., Jr., Hoogenraad, C.C., and Akhmanova, A. (2008). STIM1 is a MT-plus-end-tracking protein involved in remodeling of the ER. Curr. Biol. *18*, 177–182.

Honnappa, S., Cutting, B., Jahnke, W., Seelig, J., and Steinmetz, M.O. (2003). Thermodynamics of the Op18/stathmin-tubulin interaction. J. Biol. Chem. *278*, 38926–38934.

Honnappa, S., John, C.M., Kostrewa, D., Winkler, F.K., and Steinmetz, M.O. (2005). Structural insights into the EB1-APC interaction. EMBO J. *24*, 261–269.

Honnappa, S., Okhrimenko, O., Jaussi, R., Jawhari, H., Jelesarov, I., Winkler, F.K., and Steinmetz, M.O. (2006). Key interaction modes of dynamic +TIP networks. Mol. Cell *23*, 663–671.

Jaworski, J., Kapitein, L.C., Gouveia, S.M., Dortland, B.R., Wulf, P.S., Grigoriev, I., Camera, P., Spangler, S.A., Di, S.P., Demmers, J., et al. (2009). Dynamic microtubules regulate dendritic spine morphology and synaptic plasticity. Neuron *61*, 85–100.

Keller, R. (2004). The Computer-Aided Resonance Assignment Tutorial (Goldau, Switzerland: Cantina Verlag).

Komarova, Y., Lansbergen, G., Galjart, N., Grosveld, F., Borisy, G.G., and Akhmanova, A. (2005). EB1 and EB3 control CLIP dissociation from the ends of growing microtubules. Mol. Biol. Cell *16*, 5334–5345.

Komarova, Y., De Groot, C.O., Grigoriev, I., Gouveia, S.M., Munteanu, E.L., Schober, J.M., Honnappa, S., Buey, R.M., Hoogenraad, C.C., Dogterom, M., et al. (2009). Mammalian end binding proteins control persistent microtubule growth. J. Cell Biol. *184*, 691–706.

Kumar, P., Lyle, K.S., Gierke, S., Matov, A., Danuser, G., and Wittmann, T. (2009). GSK3beta phosphorylation modulates CLASP-microtubule association and lamella microtubule attachment. J. Cell Biol. *184*, 895–908.

Lan, W., Zhang, X., Kline-Smith, S.L., Rosasco, S.E., Barrett-Wilt, G.A., Shabanowitz, J., Hunt, D.F., Walczak, C.E., and Stukenberg, P.T. (2004). Aurora B phosphorylates centromeric MCAK and regulates its localization and microtubule depolymerization activity. Curr. Biol. *14*, 273–286.

Mimori-Kiyosue, Y., Shiina, N., and Tsukita, S. (2000). The dynamic behavior of the APC-binding protein EB1 on the distal ends of microtubules. Curr. Biol. *10*, 865–868.

Mimori-Kiyosue, Y., Grigoriev, I., Lansbergen, G., Sasaki, H., Matsui, C., Severin, F., Galjart, N., Grosveld, F., Vorobjev, I., Tsukita, S., and Akhmanova, A. (2005). CLASP1 and CLASP2 bind to EB1 and regulate microtubule plus-end dynamics at the cell cortex. J. Cell Biol. *168*, 141–153.

Mishima, M., Maesaki, R., Kasa, M., Watanabe, T., Fukata, M., Kaibuchi, K., and Hakoshima, T. (2007). Structural basis for tubulin recognition by cytoplasmic linker protein 170 and its autoinhibition. Proc. Natl. Acad. Sci. USA *104*, 10346–10351.

Moore, A.T., Rankin, K.E., von Dassow, G., Peris, L., Wagenbach, M., Ovechkina, Y., Andrieux, A., Job, D., and Wordeman, L. (2005). MCAK associates with the tips of polymerizing microtubules. J. Cell Biol. *169*, 391–397.

Nathke, I.S. (2004). The adenomatous polyposis coli protein: the Achilles heel of the gut epithelium. Annu. Rev. Cell Dev. Biol. *20*, 337–366.

Neduva, V., Linding, R., Su-Angrand, I., Stark, A., de Masi, F., Gibson, T.J., Lewis, J., Serrano, L., and Russell, R.B. (2005). Systematic discovery of new recognition peptides mediating protein interaction networks. PLoS Biol. *3*, e405.

Sandblad, L., Busch, K.E., Tittmann, P., Gross, H., Brunner, D., and Hoenger, A. (2006). The *Schizosaccharomyces pombe* EB1 homolog Mal3p binds and stabilizes the microtubule lattice seam. Cell *127*, 1415–1424.

Schuyler, S.C., and Pellman, D. (2001). Microtubule "plus-end-tracking proteins": The end is just the beginning. Cell *105*, 421–424.

Slep, K.C., Rogers, S.L., Elliott, S.L., Ohkura, H., Kolodziej, P.A., and Vale, R.D. (2005). Structural determinants for EB1-mediated recruitment of APC and spectraplakins to the microtubule plus end. J. Cell Biol. *168*, 587–598.

Steinmetz, M.O., and Akhmanova, A. (2008). Capturing protein tails by CAP-Gly domains. Trends Biochem. Sci. *33*, 535–545.

Steinmetz, M.O., Jelesarov, I., Matousek, W.M., Honnappa, S., Jahnke, W., Missimer, J.H., Frank, S., Alexandrescu, A.T., and Kammerer, R.A. (2007). Molecular basis of coiled-coil formation. Proc. Natl. Acad. Sci. USA *104*, 7062–7067.

Vitre, B., Coquelle, F.M., Heichette, C., Garnier, C., Chretien, D., and Arnal, I. (2008). EB1 regulates microtubule dynamics and tubulin sheet closure in vitro. Nat. Cell Biol. *10*, 415–421.

Weisbrich, A., Honnappa, S., Jaussi, R., Okhrimenko, O., Frey, D., Jelesarov, I., Akhmanova, A., and Steinmetz, M.O. (2007). Structure-function relationship of CAP-Gly domains. Nat. Struct. Mol. Biol. *14*, 959–967.

Wen, Y., Eng, C.H., Schmoranzer, J., Cabrera-Poch, N., Morris, E.J., Chen, M., Wallar, B.J., Alberts, A.S., and Gundersen, G.G. (2004). EB1 and APC bind to mDia to stabilize microtubules downstream of Rho and promote cell migration. Nat. Cell Biol. *6*, 820–830.

Wider, G., and Dreier, L. (2006). Measuring protein concentrations by NMR spectroscopy. J. Am. Chem. Soc. *128*, 2571–2576.

Zwahlen, C., Legault, P., Vincent, S.J.F., Greenblatt, J., Konrat, R., and Kay, L.E. (1997). Methods for measurement of intermolecular NOEs by multinuclear NMR spectroscopy: Application to a bacteriophage l N-peptide/boxB RNA complex. J. Am. Chem. Soc. USA *119*, 6711–6721.